Potassium-Dependent Folding: A Key to Intracellular Delivery of G-Quartet Oligonucleotides as HIV Inhibitors†

Naijie Jing,*,‡ Weijun Xiong,‡ Yongli Guan,‡ Luke Pallansch,§ and Shimei Wang‡

Infectious Diseases Division, Department of Medicine, Baylor College of Medicine, Houston, Texas 77030, and Southern Research Institute, Frederick, Maryland 21701

Received November 9, 2001

ABSTRACT: Several groups have demonstrated that G-rich oligonucleotides forming G-quartet structures display activity as potential drugs, such as potent HIV inhibitors. The delivery of G-quartet oligonucleotides to their intracellular targets is a key obstacle to overcome for their clinical success. Here we have developed a novel system to deliver G-rich oligonucleotides into the cell nucleus, e.g., the site of HIV integration. On the basis of the property of potassium-induced formation of G-quartet structure, we explored the difference of K^+ concentrations inside (140 mM) and outside (4 mM) cells to induce the G-rich oligonucleotides to form different structures inside and outside cells. The key steps of this delivery system include the following: (i) First, the G-quartet structure is denatured to form a lipid−DNA complex, so that the molecules can be well delivered into cells. (ii) Then the delivered molecules are induced to form G-quartet structures by potassium inside cells since the G-quartet structure is the primary requirement for inhibition of HIV-1 HIV integrase (IN) activity. The molecules of a novel G-quartet HIV inhibitor, T40214, with the sequence of $(GGGC)_4$ were successfully delivered into the nuclei of target cells, which significantly decreased HIV-1 replication and increased the probability to target HIV-1 IN in infected cells.

The G-rich oligonucleotides have been identified, cloned, and characterized in the telomeric sequences of many organisms, such as fungi, ciliates, vertebrates, and insects (*1*). The main structural motif of telomeric DNA is the G-quartet structure, which was first proposed by Cellert et al. (*2*). The G-quartet consists of four guanine bases in a sequence array arranged into a cyclic Hoogsteen H-bonding structure, and each G-base makes two H-bonds with its neighbor G-base (N1 to O6 and N2 to N7). G-quartets stack on top of each other to form tetrad helical structures. The unique structural feature of the G-quartet is a pocket in the center lined by electronegative carbonyl oxygens to be the site of interaction with a cation. G-quartet structures exhibit some specific behaviors as nucleic acids (*3*−*5*). They are very polymorphic. A family of related G-quartet structures, such as a single-stranded monomer, hairpin dimers, and parallel-stranded tetramers, can be formed on the basis of sequence, concentration, and base composition of the nucleic acids. Also, they can readily discriminate between different monovalent cations. G-tetrad-forming oligonucleotides have specific affinity for monovalent cations, and G-quartet formation strongly depends on the presence of cations. The order of preference that has been proposed is $K^+ > Rb^+ > Na^+ > Li^+$ or Cs^+ (*6*, *7*). The selectivity of G-quartet structures for cations is due to the ionic radius, and potassium appears to have the optimal size to interact within a G-octamer. The folding and unfolding transitions for G-quartet structures are extremely slow, so that the G-quartet structures are both thermodynamically and kinetically stable. The stability and slow kinetic transition of G-quartet structures have some important consequences for their biological rules.

HIV integrase (IN) has recently attracted much attention as a drug target since integration of viral DNA into the host cell chromosome is essential for HIV-1 replication. The major steps involved are (i) 3′ processing, nicking of 3′-ends of viral DNA adjacent to highly conserved CA dinucleotides, and (ii) strand transfer, insertion of the 3′-ends of precleaved viral DNA into both strands of the host DNA (*8*, *9*). The G-rich oligonucleotides were recently demonstrated to inhibit HIV-1 IN by forming an intramolecular G-quartet structure (*10*−*12*), acting by a mechanism different from antisense oligonucleotides (*13*). Also, several groups have shown that compounds containing G-quartet structures display activity as potential drugs (*14*, *15*). The delivery of G-quartet oligonucelotides to the designed targets is a critical issue for oligonucleotides as phamarceuticals. In the presence of K^+ ions, a G-rich oligonucleotide, T30695 (or T30923), with the sequence of $(GGGT)_4$ was determined to form a symmetric and compact intramolecular G-quartet, and its folded loop domains greatly increase the structural stability (*16*, *17*). The intramolecular G-quartet structure is the primary requirement for inhibition of HIV-1 IN in vitro and the inhibition of HIV-1 replication in infected cells (*12*). To utilize this structure as an antiviral, we have developed a novel system to deliver G-quartet oligonucleotides into the nuclei of target cells, e.g., the site of HIV integration.

EXPERIMEMTAL PROCEDURES

Oligonucleotide Synthesis. All of the G-rich oligonucleotides, including 5′-biotin-labeled oligonucleotides, were

† This work was supported by NIH Grant GM 60153.

* To whom correspondence should be addressed. Phone: (713) 798-3685. Fax: (713) 798-8948. E-mail: njing@bcm.tmc.edu.

‡ Baylor College of Medicine.

§ Southern Research Institute.

10.1021/bi0120401 CCC: $22.00
Published on Web 04/06/2002

synthesized by Midland Certified Reagent Co. (Midland, TX). Lipofectin reagent was obtained from Life Technologies.

Circular Dichroism. CD spectra of the G-quartet oligonucleotides were obtained in 15 μM strand concentration in 10 mM KCl and 20 mM Li_3PO_4, at pH 7, on a Jasco J-500A spectropolarimeter at room temperature. Each spectrum is represented by five average scans, and data are presented in molar ellipticity ($deg \cdot cm^2 \cdot dmol^{-1}$).

Kinetic Measurement. Folding kinetics were obtained with the manual addition of metal ions at $t = 0$, followed by absorption measurement at 264 nm, using a hp 8452A UV spectrophotometer. Mixing dead time was about 5 s. Kinetics were monitored from 5 s to 15 min. The folding time constants, τ_1 and τ_2, were estimated by fitting the UV kinetic curves using the function of a sum of two exponentials, i.e., $A(t) = A_o[\exp(-t/\tau_2) - f \exp(-t/\tau_1)]$, where $A_o = C\epsilon l$, C is the total concentration of oligonucleotide, ϵ is the extinction coefficient of the oligonucleotide sequence, l is the path length, and f is the fitting constant.

Gel Electrophoresis. (A) The oligonucleotides T30923 and T40214 in 10 mM KCl and 20 mM Li_3PO_4 were heated at 90 °C for 15 min and then cooled at 4 °C for 1 h for formation of the G-quartet structure. (B) T30923 and T40214 in H_2O were heated at 90 °C for 30 min and then gradually cooled to room temperature for denatured oligonucleotides. The oligonucleotides in both the G-quartet structure and the unfolded state were labeled with ^{32}P using the 5′-end-labeling procedure and purified using G-25 spin columns. Lipofectin was added in the labeled samples at a designated ratio to form lipid−DNA complexes. Then lipid−DNA complexes were vortexed and incubated at room temperature for 30 min. The 20% nondenaturing polyacrylamide gels were precooled in a 4 °C cold room in 1 × TBE buffer for 1 h. Then the samples with or without lipid were loaded into the gels, and the gels were run in the cold room.

Lipid−DNA Delivery Tests. (A) Nondenaturing Gel. The following procedure was used: (1) incubate ^{32}P-labeled oligonucleotides, in the denatured state and in the G-quartet structure, with lipofectin at a ratio of lipid:oligo of 5:1 at room temperature for 1 h and then add 350 ng of the ^{32}P-labeled oligonucleotides into each cell culture plate containing about 3×10^5 cells; (2) incubate the lipid−DNA complexes with cells at 37 °C for 24 h; (3) pour off the cell growth medium; (4) wash the cell plates three times with PBS to remove the oligonucleotides outside of cells and attached to cells; (5) collect the cells in a tube and lyse the cells with lysis buffer; (6) spin down the lysed samples at 15000 rpm for 15 min to separate the oligonucleotides from cell debris; (7) add 2.5 volumes of 100% ethyl alcohol in the supernatant to precipitate the ^{32}P-labeled oligonucleotides; (8) dry the pellets after centrifuging the precipitated oligonucleotides at 15000 rpm for 15 min again; (9) load the resuspended pellets in a 20% nondenaturing polyacrylamide gel and run the gel at 4 °C.

(B) Microscopy. The following procedure was used: (1) incubate 5′-biotin-labeled oligonucleotides, T40214 and T30923, with lipofectin at a ratio of lipid:oligo of 5:1 at room temperature for 1 h and then add 350 ng of the labeled oligonucleotides to each cell plate; (2) incubate the lipid−DNA complexes with cells at 37 °C for 24 h; (3) remove the cell culture medium and wash the plates three times with PBS; (4) lyse the cells for 2 min by adding 0.5% Triton and fix the lysed cells on slides for 15 min in 3.7% formaldehyde; (5) develop dye fluorescence in the 5′-biotin-labeled oligonucleotides by incubating at room temperature for 1 h using Avidin Texas Red; (6) wash the cells three times with PBS to eliminate free fluorescence; (7) identify the G-quartet oligonucleotides under microscopy.

Assay of Anti-HIV-1 Integrase Activity. The following oligonucleotides were purchased from Midland Certified Reagent Co. (Midland, TX): 19-mer, 5′-GTGTGGAAATCTCTTAGCA; 21-mer, ACTGCTAGAGATTTTCCACAC. The HIV-1 IN(F185K/C280S) was obtained from the AIDS Research and Reference Reagent Program, NIH. The oligonucleotide was labeled by [γ-^{32}P]ATP using T_4 polynucleotide kinase. The mixture of the two oligonucleotides was heated at 95 °C, allowed to cool slowly to room temperature, and run on a G-25 spin column to separate annealed double-stranded oligonucleotide from unincorporated label. In the strand transfer assay, HIV-1 IN was preincubated at a final concentration of 400 ng with G-quartet inhibitors for 15 min at 30 °C in a reaction buffer containing 25 mM MOPS, pH 7.2, 25 mM NaCl, 7.5 mM $MnCl_2$, 0.1 mg/mL BSA, and 14.3 mM β-mercaptoethanol. Then 5 nM 5′-end ^{32}P-labeled duplex oligonucleotides were added to the final volume of 10 μL, and incubation was continued for an additional 1 h. Reactions were quenched by addition of 5 μL of denaturing loading dye. Samples were loaded on a 20% (19:1) denaturing polyacrylamide gel.

Evaluation of Anti-HIV Efficacy in Cell Lines. Uninfected CEMSS cells were passaged in T-150 flasks for use in the assay. On the day preceding the assay, the cells were split 1:2 and washed twice in tissue culture medium and resuspended in fresh medium. Cell viability must be greater than 95% for the cells to be utilized in the assay. The cells were pelleted and resuspended at 2.5×10^4 cells/mL in tissue culture medium and added to the drug-containing plates in volumes of 50 μL. A pretitered aliquot of HIV-1 (RF strain) was then resuspended and diluted into tissue culture medium. An amount of virus (or virus plus inhibitors) was added to each well in a volume of 50 μL to measure cell killing at postinfection for 6 days. After 6 days of incubation at 37 °C in a 5% CO_2 incubator, the test plates were analyzed by macroscopic observation, using staining with the tetrazolium dye XTT. The results of the macroscopic observation were confirmed by further microscopic analysis to evaluate the activity of the test compounds. XTT solution was prepared daily as a stock of 1 mg/mL in PBS. Phenazine methosulfate solution (PMS) was prepared at 15 mg/mL in PBS and stored in the dark at −20 °C. XTT/PMS stock was prepared immediately before use by diluting the PMS 1:100 in PBS and adding 40 μL/mL of XTT solution. Then 50 μL of XTT/PMS was added to each well of the plate, and the plate was incubated at 37 °C for 4 h. Adhesive plate sealers were used instead of the lids, the sealed plate was inverted several times to mix the soluble formazan product, and the plate was read by a spectrophotometer (Molecular Devices Vmax plate reader) at 450 nm. The results of EC_{50} were calculated and plotted as percent inhibition of HIV replication verse drug concentration.

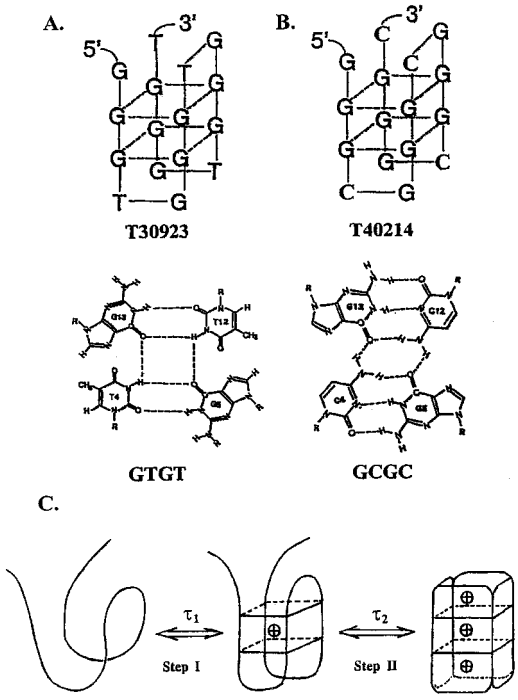

FIGURE 1: G-quartet models and H-bond formations of loop structures of T30923 (A) and T40214 (B). (C) Two-step kinetic model of K^+-induced folding of G-quartet oligonucleotides, which has been identified previously by NMR and UV kinetics (see text for details).

RESULTS

Structure and Folding Kinetics of T30923 and T40214. The G-quartet oligonucleotides as HIV inhibitors used in this delivery study were T30923 and T40214 with the sequences of $(GGGT)_4$ and $(GGGC)_4$, respectively. T30923 forms an intramolecular G-quartet structure with two G-quartets in the middle and two G-T-G-T loops on the top and bottom determined by NMR (*17*) (Figure 1A). Further evidence to support intramolecular G-quartet formation for T30923 was obtained from nondenaturing gel electrophoresis and from melting and annealing measurements (*18*). T40214 is a newly designed HIV inhibitor and is expected to form an intramolecular G-quartet structure with two G-quartets in the middle and two G-C-G-C loops on the top and bottom (Figure 1B). CD spectra demonstrated that T40214 forms the same intramolecular G-quartet structure as T30923 (Figure 2).

Our previous NMR data demonstrated (*16*, *17*) that T30923 folds to an intramolecular G-quartet structure in two steps from the open state (Li^+ form) to the closed state (K^+ form) by binding three K^+ ions. The first step corresponds to a rearrangement of the bases of the two central G-quartets during the binding to a K^+ ion, and the second step results from the loop base folding parallel to the bases of the underlying G-quartet by binding an additional K^+ between a G-quartet and the adjacent loop domain on the top or bottom (Figure 1C). The kinetics of UV absorption versus time showed that the structure transition of T30923 was also composed of two steps, corresponding to the two-step transition observed by NMR. The first step is hyperchromic and the second one is hypochromic in UV absorption, respectively. The kinetics of K^+-induced structure folding for T30923 and T40214 are shown in Figure 3. At K^+ concentrations of 0.05 and 8.0 mM (Figure 3A,C), the time

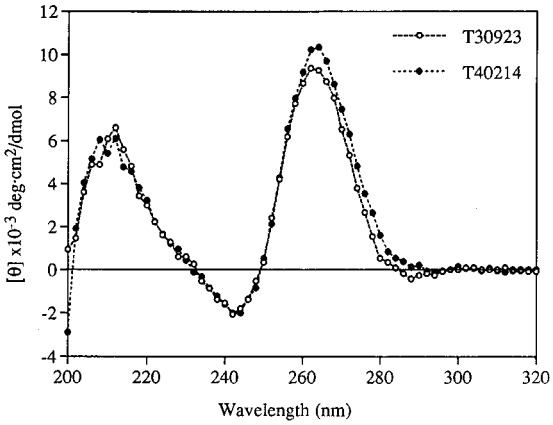

FIGURE 2: CD spectra of T40213 and T30923 showing that the two oligonucleitdes form the same intramolecular G-quartet structure. A stable G-quartet structure is characterized by a CD spectrum with maxima at 264 and 210 nm and a minimum at 240 nm.

constants (τ_1) of the first step are about 5 and 6 s for T30923 and T40214 while the time constants (τ_2) of the second step are about 10^4-10^5 s for T30923 and T40214. The large time constants of τ_2 indicate no second step occurring in these K^+ concentrations. When the K^+ concentrations were raised to 5.0 and 50.0 mM, respectively (Figure 3B,D), the first step became too rapid to be observed with our instruments, and the time constants (τ_2) of the second step decreased to 22 s for T30923 and 32 s for T40214. The decrease in UV absorption in the second step (Figure 3B,D) was caused by an increase in DNA base stacking because the loop bases folded parallel to the bases of the underlying G-quartet to form a compact G-quartet structure. Although both T30923 and T40214 were shown to form the same G-quartet structure, the significant difference of folding kinetics between the two oligonucleotides was the concentration of potassium inducing the oligonucleotides to form the G-quartet structure. The first step for T30923 was observed in 0.05 mM KCl while that of T40214 occurred in 8.0 mM KCl. At 5.0 mM KCl, T30923 formed a compact G-quartet structure with two folded loop domains; however, T40214 formed the same structure at 50 mM KCl. T40214 has a much weaker binding affinity to K^+ ions than T30923. The loop domain of T40214 was expected to form H-bonds as shown in Figure 1B when an additional K^+ coordinated between a G-quartet and the adjacent loop domain. However, our modeling study predicted that the G-C-G-C loop domain of T40214 cannot fold into a plane because of the short distance between C-G bases, which may cause a decrease in the binding affinity to K^+ ions (data not shown).

Formation of Lipid−DNA Complexes. Nondenaturing electrophoresis was employed for the delivery study, in which the migrational rate of an oligonucleotide depends on the size of its molecular structure. The different rates of migration of the oligonucleotide in a nondenaturing gel correspond to different molecular structures. The gel of T30923 (Figure 4A) showed that the intensity of the bottom band, which corresponds to the molecules in the G-quartet structure, remained unchanged when T30923 was mixed with lipofectin at a ratio of oligo:lipid from 1:0 to 1:10. Lipofectin is composed of 1:1 (w/w) liposome formulation of the cationic lipid *N*-[1-(2,3-dioleyloxy)propyl]-*N*,*N*,*N*-trimenthylammonium chloride (DOTMA) and dioleoylphosphatidylethanolamine (DOPE). The faint bands at the top of the

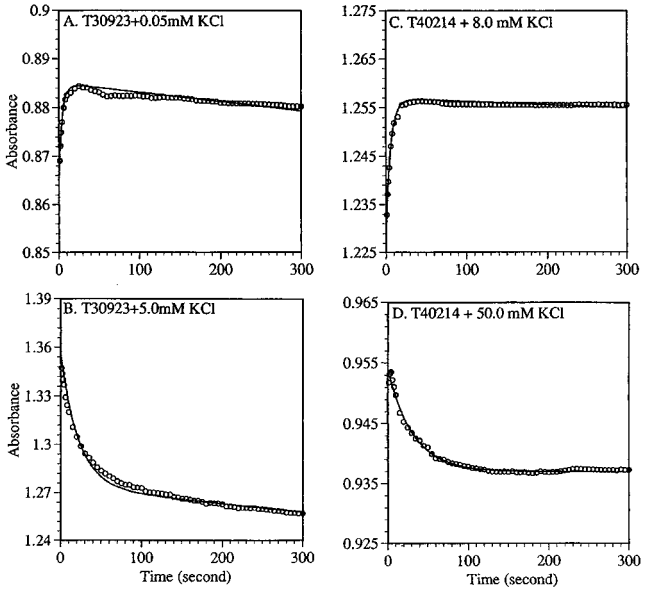

FIGURE 3: Kinetics of the K^+-induced structure transition of G-quartet oligonucleotides. Plots are presented in UV absorbance at 264 nm versus time after addition of K^+ ions. The kinetic curves for T30923 and T40214 were obtained at 0.05, 5.0, 8.0, and 50.0 mM KCl, respectively. The curves were fitted by a sum of two exponentials, i.e., $A(t) = A_0[\exp(-t/\tau_2) - f\exp(-t/\tau_1)]$, and the folding time constants, τ_1 and τ_2, were obtained from the fittings.

gel corresponded to the molecules of oligonucleotides incorporated with lipid to form lipid−DNA complexes, which have a large size with slow migration (Figure 4A). A significant difference was observed in Figure 4B,C when T30923 and T40214 were totally denatured. Thus, no G-quartet band appeared at the bottom of the gels in Figure 4B,C. An intensive band corresponding to lipid−DNA complexes appeared at the top of the gels when the ratio of oligo:lipid was raised from 1:1 to 1:20. Clearly, the denatured molecules of T30923 and T40214 readily incorporate within lipid micelles to form lipid−DNA complexes. On the basis of the analysis of the intensities of the two bands, the top and the middle bands in each lane, we found that more than 60% of the denatured DNA molecules were incorporated into lipid micelles when the lipid:oligo ratio reached 2:1 for T40214 and 5:1 for T30923 (Figure 5). These data demonstrate that only the G-rich oligonucleotides in the unfolded state can incorporate well within liposomes to form a lipid−DNA complex; however, the oligonucleotides in the G-quartet structure are barely able to form lipid−DNA complexes with liposomes.

Intracellular Delivery of G-Quartet Oligonucleotides. Figure 6 demonstrated that the molecules of T40214 and T30923 were delivered into cells by lipid−DNA complexes. The same amounts (350 ng) of ^{32}P-labeled oligonucleotides, T40214 and T30923, in the unfolded state and in the G-quartet structure were incorporated into lipofection at a ratio of lipid:oligo of 5:1. Then they were incubated in cell plates for 24 h at 37 °C, and each plate contained about 3×10^5 cells. Lanes 2−5 of the gel were loaded by the labeled oligonucleotides after they were extracted from inside cells (see Experimental Procedures for details). Lane 1 is T40214 in the G-quartet structure without lipid as a control. Lanes 2 and 4 were the molecules of T40214 delivered in the unfolded state and in the G-quartet structure, respectively. Lanes 3 and 5 were the same strategy for T30923. Compared with the band in lane 1, the bands at the bottom in lanes 2−5 correspond to the molecules re-formed to the G-quartet structure inside cells and the bands at the top showed the molecules maintaining in lipid−DNA complexes. On the basis of the analysis of the intensities of the two bands from lane 2 to lane 5, we found the following: (1) The total molecules of T30923 (lane 3) delivered inside cells is only 47% of that of T40214 (lane 2). The efficiency of delivering T30923 is much lower than that of T40214. (2) The total molecules of T40214 delivered in the G-quartet structure (lane 4) is about 40% of that delivered in the unfolded state (lane 2) since the molecules in the G-quartet structure have a low ratio to form lipid−DNA complexes with lipid. (3) Compared with the intensities of the two bands in lane 2, about 50% of the total molecules of T40214 inside cells were released from the DNA−lipid complex to re-form the G-quartet structures in 24 h, induced by potassium inside cells.

Stained cells showing oligonucleotide delivery are demonstrated in Figure 7. The biotin-labeled oligonucleotide molecules were dyed in red, and the nuclei of cells were counterstained in blue. The color of nuclei turned to pink when oligonucleotide molecules entered into the nuclei. The data were obtained after the lipid−DNA complexes of T40214 and T30923 were incubated with the cells at 37 °C for 24 h. The deliveries for T40214 and T30923 in the unfolded state were tested in different cell lines, such as 3T3 (A and B), CEMSS (C and D), and MT4 (E and F) cells, respectively. The pictures show that much larger amounts of T40214 molecules than T30923 molecules in the unfolded state were transported inside cells and nuclei in different cell lines (Figure 7A−F). No oligonucleotide molecules of T40214 and T30923 in the G-quartet structure were observed in the cells (Figure 7G,H), showing that the G-quartet oligonucleotides without lipid deliverers cannot penetrate into cells. The results observed in Figure 7 are consistent with those in Figure 6. The delivery efficiency of G-rich oligonucleotides not only strongly depends on molecular structure, G-quartet or unfolded, but also depends on sequences of G-rich oligonucleotides.

Effective Intracellular Delivery System. The results showed clearly that lipid deliverers only can form lipid−DNA complexes with unfolded molecules of the G-rich oligonucleotides (Figure 4), and also the molecules in the G-quartet structure cannot penetrate cell membranes directly to reach their target inside cells (Figure 7G,H). On the basis of the property of potassium-induced formation of the G-quartet structure, we explored the difference of K^+ concentrations inside (140 mM) and outside (4 mM) cells to induce the G-rich oligonucleotides to form a different structure inside and outside cells. A novel intracellular delivery system for G-quartet oligonucleotides was proposed in Figure 8. This system includes several steps: (i) G-quartet oligonucleotides are denatured in order to increase the probability of incorporation of G-rich oligonucleotides within lipid. (ii) The denatured molecules are mixed with lipid to form lipid−DNA complexes. (iii) The lipid−DNA complexes are incubated with cells. (iv) Then the delivered molecules refold to form to G-quartet structure, induced by the action of K^+ ions inside cells.

Enhancement of the Inhibition of HIV-1 Replication by Intracellular Delivery. The inhibitions of HIV-1 IN on strand

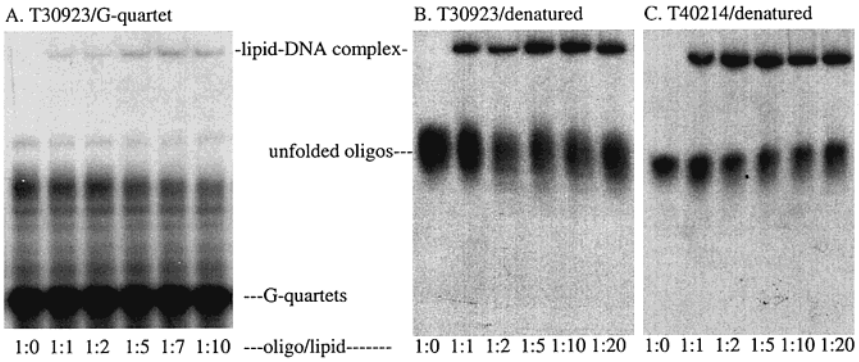

FIGURE 4: Nondenaturing gels. (A) T30923 in the G-quartet structure was mixed with lipofectin at a ratio of oligo:lipid from 1:0 to 1:10; (B and C) T30923 and T40214 in the denatured state were incorporated with lipofectin at a ratio of oligo:lipid from 1:0 to 1:20, respectively.

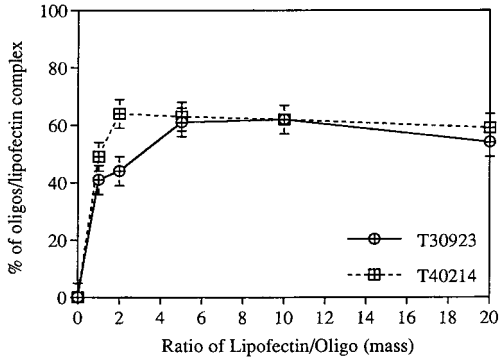

FIGURE 5: Plots obtained on the basis of the ratio of the intensities of the top band to that of the top band plus the middle band in Figure 4B,C versus the ratio of lipofection:oligo in mass. The plots show that more than 60% of the total DNA molecules were incorporated with lipofectin to form lipid−DNA complexes when the ratio of lipid:oligo reached to 2:1 for T40214 and 5:1 for T30923.

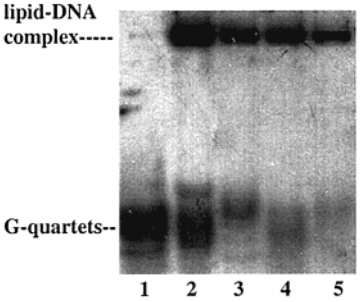

FIGURE 6: A nondenaturing gel shows that the molecules of T40214 and T30923 were delivered inside cells by lipid−DNA complexes. Lane 1 is T40214 in the G-quartet structure without lipid as a control. Lanes 2−5 were loaded by ^{32}P-labeled oligonucleotides extracted from inside cells after the oligonucleotides were incubated with cells for 24 h at 37 °C. Lanes 2 and 4 show the molecules of T40214 delivered in the unfolded state and in the G-quartet structure, respectively. Lanes 3 and 5 show the molecules of T30923 delivered in the unfolded state and in the G-quartet structure, respectively.

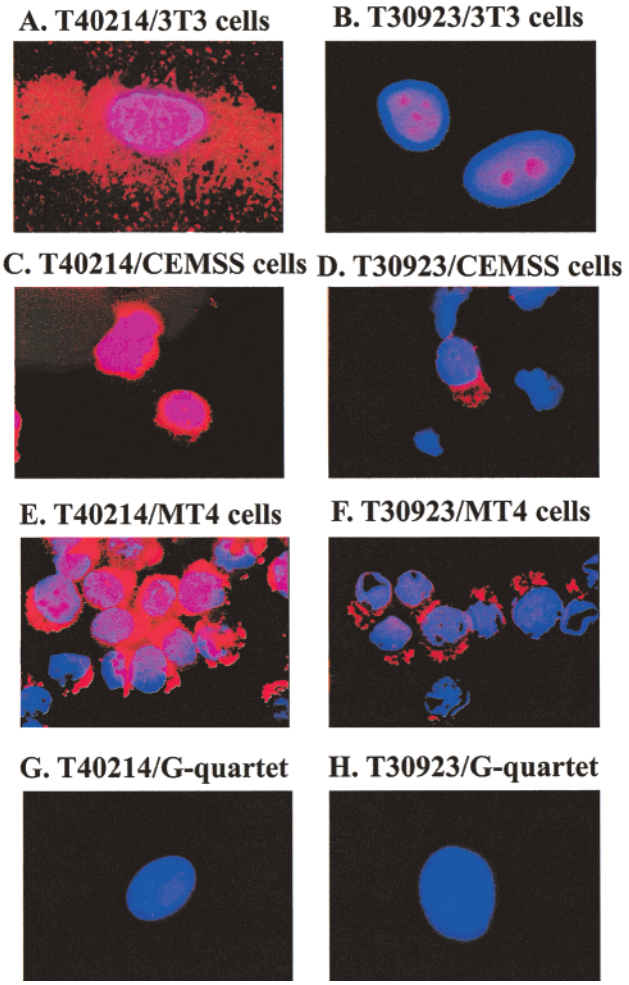

FIGURE 7: Demonstration of the biotin-labeled molecules of T40214 and T30923 delivered into cells and nuclei. The biotin-labeled oligonucleotide molecules are dyed red, and the nuclei of cells are counterstained blue. The color of the nuclei turned to pink when oligonucleotide molecules entered into the nuclei. The biotin-labeled oligonucleotide molecules were delivered in the unfolded state with lipofectin at a ratio of oligo:lipid of 1:5 (A−F) and in G-quartet structure without lipofectin (G and H).

transfer for T30923 and T40214 were measured in a dual assay, which detected the disintegration of HIV-1 IN (Figure 9A). The procedure of integration of the cleaved viral DNA into host DNA by HIV-1 IN is referred to as strand transfer (ST). In lanes 1 and 8, the strong bands correspond to the duplex oligonucleotide without HIV-1 IN as controls. ST products, which are from joining the 3′-end of one duplex to another, yield larger molecular species with slower migration. The intensities of the ST bands significantly decreased when the concentration of the G-quartets increased from 0 to 500 nM. IC_{50}s of the inhibition of ST of HIV-1 IN for T30923 and T40214 are 80 and 40 nM, respectively (Figure 9A). The two oligonucleotides have a comparable capacity to inhibit HIV-1 IN activity in vitro. Figure 9B shows plots of inhibition of HIV-1 (RF) replication versus drug concentration for T40214, T30923, T40208, and

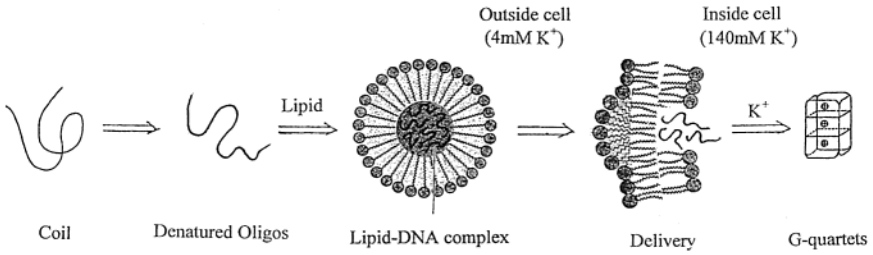

FIGURE 8: Scheme of the intracellular delivery system for G-quartet oligonucleotides.

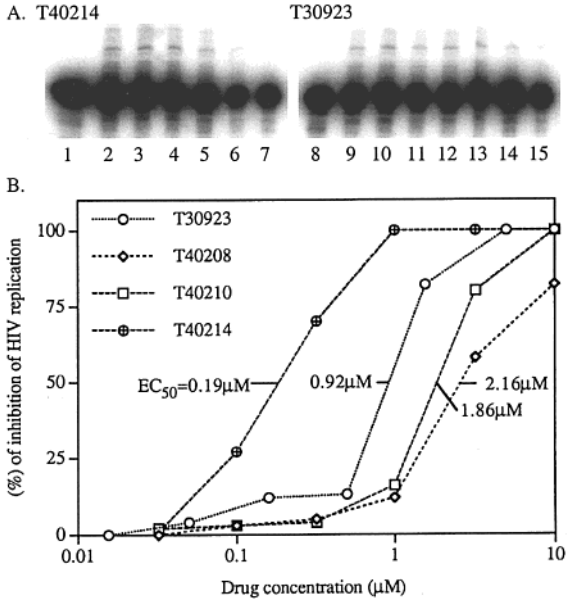

FIGURE 9: Results demonstrating the inhibition of strand transfer (ST) on HIV-1 IN in vitro (A) and the inhibition of HIV-1 (RF) replication in CEMSS infected cells (B). Lanes 1 and 8 indicate duplex DNA as controls. Compared with lanes 1 and 8, ST products yield larger molecular species with slower migration. The intensity of the ST band significantly decreased when the concentration of G-quartets increased from 0, 1, 5, 10, 50, 100, and 500 nM. IC_{50}s of T30923 and T40214 are 80 and 40 nM, respectively. Plot B shows the inhibition of HIV-1 replication in CEMSS cells by lipid-delivered T30923, T40214, T40208, and T40210. EC_{50}s of the inhibition of HIV-1 (RF) replication in CEMSS cells for T40214, T30923, T40208, and T40210 are 0.19, 0.92, 2.16, and 1.86 μM, respectively (see text for details).

T40210 in CEMSS infected cells. The G-rich oligonucleotides of T40208 (GGGCGGGTGGGTGGGT) and T40210 (GGGTGGGTGGGCGGGT) were used as nonspecific controls. Each data point was the average of six measured values. EC_{50}s of the inhibition of HIV-1 (RF) replication for T40214 and T30923 in infected cells are 0.19 and 0.92 μM, respectively. The EC_{50} of T40214 is 5-fold lower than that of T30923. The significant difference of the inhibition of HIV replication between the two oligonucleotides is most likely caused by their intracellular delivery. The high efficiency of intracellular delivery for T40214 greatly deceases HIV-1 replication and increases the probability to target HIV-1 IN in infected cells. T40208 and T40210 were composed by the substitution of a single cytosine for a thymine at residues 4 and 12 of T30923, respectively. These substitutions strongly disrupted the T4-G5-T12-G13 loop structure of T30923 (Figure 1A), so that they cannot form a compact intramolecular G-quartet structure. The factor that the inhibition of HIV-1 (RF) replication for T40208 (EC_{50} = 2.16 μM) and T40210 (EC_{50} = 1.86 μM) is much weaker than that of T40214 provides the evidence that re-forming the G-quartet structure of T40214 inside cells is also very important for the inhibition of HIV replication.

DISCUSSION

The difficulties to develop an effective delivery system for G-quartet-forming oligonucleotides mainly come from their physical and structural properties. T30923 forms a stable and symmetric intramolecular G-quartet structure with about 15 Å width and 15 Å length in the presence of K^+ ions (*17*). This structure seems to resemble a cylinder with positive charges inside and negative charges on the surface. The net charge on the T30923/K^+ complex is most likely to be close to a neutral zwitterion under physiologic conditions. All cationic lipids are composed of three parts: a hydrophobic anchor, a linker, and a headgroup. Double-chain hydrocarbons represent the majority of cationic lipids. Electrostatic interaction is the primary driving force for binding of lipid−DNA complexes to the cell membrane. The transfection efficiency of a given lipid−DNA complex depends on its structural and physicochemical properties (*19*, *20*). Generally, the charge of the complexes is slightly positive to allow interaction with negatively charged cell surfaces, thus increasing the cellular uptake. G-quartets with neutral charge barely incorporate into cationic liposome.

The important development in this study is that, on the basis of the property of potassium-dependent formation of the G-quartet structure, we use the difference of K^+ concentrations inside and outside cells to induce the molecules of G-rich oligonnucleotides forming different structures inside and outside cells, so that to establish an effective intracellular delivery system for the G-quartet oligonucleotides. The data showed that the efficiency of intracellular delivery for T40214 is much higher than that for T30923. The difference between the two oligonucleotides is the substitution of the residues of cytosine for the residues of thymine in T40214 loop domains. The substitution was designed to greatly decrease the binding affinity of T40214 to K^+ ions. Generally, the K^+ ion concentration is 4 mM outside cells and 140 mM inside cells (*21*). T30923 folds to a compact G-quartet at 5.0 mM KCl; however, T40214 folds to the same G-quartet structure at 50.0 mM KCl. The T30923 cannot be well delivered into cells because T30923 molecules refold to the G-quartet structure outside of cells. The high delivery efficiency for T40214 results from the fact that the molecules maintain the unfolded structure before entering cells.

Intracellular delivery of G-quartet oligonucleotides by DNA−lipid complexes can be divided into three steps: (1) binding and internalization of DNA by the cells, (2) escape of the DNA into the cytoplasm, and (3) entry of the DNA

oligonucleotides into the nucleus. The primary driving force for the binding of the lipid−DNA complex to the cell membrane is electrostatic (*19*, *20*). The internalization of the lipid−DNA occurs mainly through endocytosis. The fact that DNA oligonucleotides are released into the cytoplasm is most likely caused by the interaction between cationic lipid and anionic molecules present in the membrane. Variation of the charge ratio, incubation time, or the component of lipids could increase the percentage and speed of DNA oligonucleotides released from lipid−DNA complexes. Entry of G-quartet oligonucleotides into the nucleus is a key obstacle to overcome since the activity of HIV-1 IN, i.e., the integration of viral DNA into host DNA, occurs in the nucleus. Our results demonstrated that molecules of T40214 successfully entered into nuclei after they were incubated in cells for 24 h. The main reason that the refolded G-quartet molecules can penetrate into the nucleus is considered to be due to their structural characters. After the oligonucleotide molecules were released from lipid−DNA complexes and entered the cytoplasm, they refolded to form G-quartet structures due to the influence of K^+ ions inside the cells. The highly stable and compact G-quartet structure greatly enhances the ability of the oligonucleotides to resist nuclease digestion (*13*). Thus the molecules re-formed to the G-quartet structure have a greater capacity to penetrate into the nucleus through the nuclear pores.

Although HIV-1 IN as a target has recently attracted much attention, the agents developed thus far are ineffective at inhibiting HIV-1 IN in infected cells (*22*−*24*). Our results indicate that the G-quartet molecules without lipid-mediated deliverers cannot penetrate cell membranes to target HIV-1 IN inside cells. These results match the previous studies (*25*, *26*), in which the G-quartet oligonucleotide, T30177, in the absence of lipid-mediated deliverers was observed to inhibit the enveloped protein gp120 on the surface of cells instead of HIV-1 IN inside cells. Failure to target HIV-1 IN within cells is probably due to its inability to penetrate the cell membrane. Our intracellular delivery system includes two critical steps: (i) denaturing the G-quartet structure in order to form a lipid−DNA complex with lipid, so that the molecules can be well delivered into cells; (ii) then inducing the delivered molecules to re-form the G-quartet structure by potassium inside cells since the G-quartet structure is the primary requirement for inhibition of HIV-1 IN activity. This efficient delivery greatly increases the probability of the intracellular inhibition of HIV-1 IN for G-quartet oligonucleotides and also provides critical information for drug design, that is, to design potent G-quartet HIV inhibitors with structure folding in potassium concentrations between 4 and 140 mM.

REFERENCES

1. Henderson, E. (1995) in *Telomeres*, pp 11−34, Cold Spring Harbor Laboratory Press, Cold Spring Harbor, NY.
2. Cellert, M., Lipsett, M. N., and Davies, D. R. (1962) *Proc. Natl. Acad. Sci. U.S.A. 48*, 2013−2018.
3. Williamson, J. R. (1994) *Annu. Rev. Biophys. Biomol. Struct. 23*, 703−730.
4. Rhodes, R., and Giraldo, R. (1995) *Curr. Opin. Struct. Biol. 5*, 311−322.
5. Gilber, D. E., and Feigon, J. (1999) *Curr. Opin. Struct. Biol. 9*, 305−314.
6. Sen, D., and Gillbert, W. (1990) *Nature 344*, 410−414.
7. Jing, N., Rando, F. R., Pommier, Y., and Hogan, M. E. (1997) *Biochemistry 36*, 12498−12505.
8. Katzman, M., and Katz, R. A. (1999) *Adv. Virus Res. 52*, 371−395.
9. Asante-Applah, E., and Skalka, A. M. (1999) *Adv. Virus Res. 52*, 351−369.
10. Rando, F. R., Ojwang, J., Elbaggari, A., Reyes, G. R., Tinder, R., McGrath, M. S., and Hogan, M. E. (1995) *J. Biol. Chem. 270*, 1754−1760.
11. Mazumder, A., Neamati, N., Ojwang, J. O., Sunder, S., Rando, R. F., and Pommier, Y. (1996) *Biochemistry 35*, 13762−13771.
12. Jing, N., De Clercq, E., Rando, F. R., Pallansch, L., Lackman-Smith, C., Lee, S., and Hogan, M. E. (2000) *J. Biol. Chem. 275*, 3421−3430.
13. Jing, N. (2000) *Expert Opin. Invest. Drugs 9* (8), 1777−1785.
14. Bock, L. C., Griffin, L. C., Latham, J. A., Vermaas, E. H., and Toole, J. J. (1992) *Nature 355*, 564−566.
15. Wyatt, J. R., Vickers, T. A., et al. (1994) *Proc. Natl. Acad. Sci. U.S.A. 91*, 1356−1360.
16. Jing, N., Gao, X., Rando, R. F., and Hogan, M. E. (1997) *J. Biomol, Struct. Dyn. 15*, 573−585.
17. Jing, N., and Hogan, M. E. (1998) *J. Biol. Chem. 273*, 34992−34999.
18. Jing, N., Marchand, C., Liu, J., Mitra, R., Hogan, M. E., and Pommier, Y. (2000) *J. Biol. Chem. 275*, 21460−21467.
19. Maurer, N., Mori, A., Palmer, L., Monck, M. A., Mok, K. W. C., Mui, B., Akhong, Q. F., and Cullis, P. R. (1999) *Mol. Membr. Biol. 16*, 129−140.
20. Chesnoy, S., and Huang, L. (2000) *Annu. Rev. Biophys. Biomol. Struct. 29*, 27−47.
21. Lodish, H., Baltimore, D., Berk, A., Zipursky, S. L., Matsudaira, P., and Darnell, J. (1995) *Molecular Cell Biology*, p 641, Scientific American Books, W. H. Freeman, New York.
22. Pommier, Y., and Neamati, N. (1999) *Adv. Virus Res. 52*, 427−459.
23. De Clercq, E. (2000) *Rev. Med. Virol. 10*, 255−277.
24. Craigie, R. (2001) *J. Biol. Chem. 276*, 23213−23216.
25. Cherepanov, P., Este, J. A., Rando, R. F., Ojwang, J. O., Reekmans, G., Steinfeld, R., David, G., De Clercq, E., and Debyser, Z. (1997) *Mol. Pharmacol. 52*, 771−780.
26. Este, J. A., Cabrera, C., Schols, D., Cherepanov, P., Gutierrez, A., Witvrouw, M., Pannecouque, C., Debyser, Z., Rando, R. F., Clotet, B., Desmyter, J., and De Clercq, E. (1998) *Mol. Pharmacol. 53*, 340−345.

BI0120401